CHEMISTRY
A EUROPEAN JOURNAL

DOI: 10.1002/chem.201000199

Rapid and Direct Conversion of Graphite Crystals into High-Yielding, Good-Quality Graphene by Supercritical Fluid Exfoliation

Dinesh Rangappa,*[a] Koji Sone,[a] Mingsheng Wang,[b] Ujjal K. Gautam,[b] Dmitri Golberg,[b] Hiroshi Itoh,[c] Masaki Ichihara,[d] and Itaru Honma*[a]

Abstract: Graphene has attracted a great deal of attention in recent years due to its unusual electronic, mechanical, and thermal properties. Exploiting graphene properties in a variety of applications requires a chemical approach for the large-scale production of high-quality, processable graphene sheets (GS), which has remained an unanswered challenge. Herein, we report a rapid one-pot supercritical fluid (SCF) exfoliation process for the production of high-quality, large-scale, and processable graphene for technological applications. Direct high-yield conversion of graphite crystals to GS is possible under SCF conditions because of the high diffusivity and solvating power of SCFs, such as ethanol, *N*-methyl-pyrrolidone (NMP), and DMF. For the first time, we report a one-pot direct conversion of graphite crystals to a high yield of graphene sheets in which about 90–95 % of the exfoliated sheets are <8 layers with approximately 6–10 % monolayers and the remaining 5–10 % are ≥ 10 layers.

Keywords: conducting materials · exfoliation · graphene · scanning probe microscopy · supercritical fluids

Introduction

Graphene has attracted a great deal of attention in recent years due to its unusual electronic, mechanical, and thermal properties. Exploiting graphene properties in a variety of applications requires a chemical approach for the large-scale production of high-quality, processable graphene sheets (GSs), which has remained an unanswered challenge. Various approaches have been developed, to date, to obtain GSs.[1,2] The standard procedure to make the high-quality graphene is the micromechanical cleavage method, which is suitable for only fundamental studies.[2] Alternatively, many researchers have reported epitaxial growth of graphene on metal or nonmetal substrates by chemical vapor deposition (CVD) or by thermal decomposition of SiC[3–5] and the graphene-type carbon materials have been produced by substrate-free CVD,[6] radio-frequency plasma-enhanced CVD,[7] aerosol pyrolysis,[8] and solvothermal synthesis.[9] On the other hand, the chemical routes are widely considered to be a promising approach for large-scale production.[10] This approach provides processable graphene that can be easily cast into various structures or integrate graphene with other materials to form nanocomposites. Currently, most of the chemical approaches based on the dispersion and exfoliation of graphene oxide or graphite intercalation compounds (GIC).[11–13] So far, the graphene derived by these methods contained a significant amount of oxygen and other functional groups with numbers of defects that cannot be restored completely.[11,12] In addition, these methods involve several steps and need 3–5 d to allow the intercalants and organic solvents to fully insert into the graphitic layers.[13]

[a] Dr. D. Rangappa, Dr. K. Sone, Prof. I. Honma
Energy Technology Research Institute
National Institute of Advanced Industrial Science and Technology (AIST), Umezono 1-1-1, Tsukuba
Ibaraki 305-8568 (Japan)
Fax: (+81)29-861-5799
E-mail: dinesh.r@aist.go.jp
i.homma@aist.go.jp

[b] Dr. M. Wang, Dr. U. K. Gautam, Prof. D. Golberg
World Premier International Center for Materials Nanoarchitectonics
National Institute for Materials Science, 1-1 Namiki
Tsukuba, Ibaraki, 305-0044 (Japan)

[c] Dr. H. Itoh
Research Institute of Instrumentation Frontier
National Institute of Advanced Industrial Science and Technology
Umezono 1-1-1, Tsukuba, Ibaraki 305-8568 (Japan)

[d] Dr. M. Ichihara
Material Design & Characterization Lab
Institute for Solid State Physics
University of Tokyo, 5-1-5, Kashiwanoha
Kashiwa, Chiba 277-8581 (Japan)

Supporting information for this article is available on the WWW under http://dx.doi.org/10.1002/chem.201000199.

Recently, Coleman and co-workers demonstrated that it is possible to effectively exfoliate graphite to produce single and few-layer GSs without the use of intercalants, if the solvents are chosen judiciously.[14] The trick was to choose solvents for which the solvent–graphene interfacial interaction energy matches that of graphene–graphene. However, the maximum yield achieved by this method was only 8.3% with a fraction of single-layer graphene among the large quantities of starting graphite material. Several rounds of sediment recycling were required to increase the yield further.

On the other hand, Gulari et al. have developed a supercritical CO_2 processing technique for intercalation and exfoliation of layered silicates and delaminating graphite structure.[15] This method consists of immersing the layered clays in supercritical CO_2 for a certain time period at a preset temperature and pressure followed by rapid depressurization. Generally, supercritical fluids (SCFs) have much more empty space than ordinary liquids and are highly compressible. Consequently, the density and hence "the solvent strength" of the fluid may be tuned from gas- to liquidlike values simply by varying pressure, temperature, or both. This tunability, along with low interfacial tension, excellent wetting of surfaces, and high diffusion coefficients, makes SCFs potentially superior solvents for diffusion between the layers and its expansion.[15]

Given the lack of a reliable approach for the large-scale and high-yield production of graphene, herein, we report a novel SCF exfoliation process to produce high-quality, gram-scale processable graphene for technological applications. Our procedure is simple and fast; it involves direct one-pot exfoliation of graphite crystals down to few (1–10)-layer GSs by SCFs, such as ethanol, *N*-methyl-pyrrolidone (NMP), and DMF. This is a noncovalent, solution-phase method to produce large scales of defect-free, unoxidized GSs.

Results and Discussion

The SCF exfoliation method resulted in a high yield of GSs in a single step. The exfoliated GSs can be dispersed well in fresh solvent and remain nonagglomerated for several days. Photographs of black solutions obtained by 5 min sonication of GS in different fresh solvents, such as DMF, ethanol, and NMP are presented in Figure 1a–c, along with the respective dried graphene powder in Figure 1d–f. The concentration of dispersed GS solutions is approximately 2–4 mg mL^{-1}. This dispersed solution was stable for several days without any stabilizers.

Solvent engineering is a very useful approach for the preparation of 1–2D carbon materials, such as carbon nanotubes (CNTs) and fullerenes.[16,17] Recently, some researchers have successfully exfoliated CNT in NMP.[17,18] Such exfoliation occurs because of the strong interaction between the solvent and the nanotube side wall, which subsidizes the energy requirement for exfoliation and subsequent solvation. Based on similar principles, Coleman and co-workers succeeded in exfoliating graphite to a few layers of graphene by using low-power sonication.[14] Although they could obtain high-quality graphene with solvent–graphene interfacial interactions, the yield was very low (≈8% with only 1% monolayer). This suggests that the surface energy of solvents matching with that of graphene is not sufficient for high-yield exfoliation of graphite down to a few layers (1–10 layers). Complete exfoliation can only occur if the net energetic cost is zero or with a solvent that has high diffusivity and high solvation power. To realize this, we dispersed

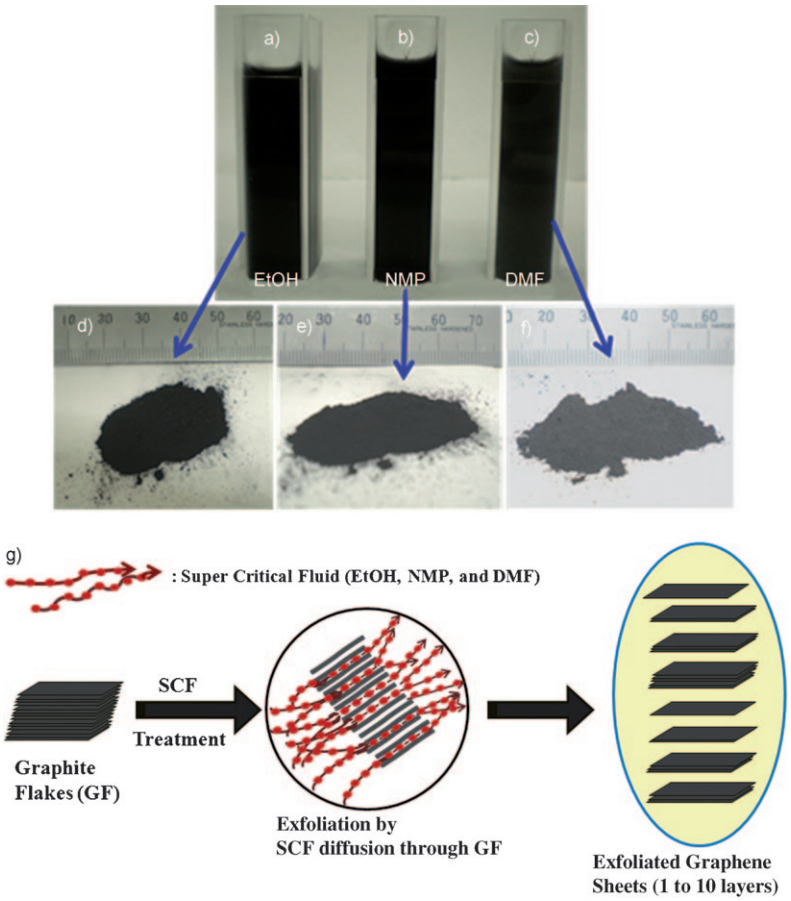

Figure 1. Photographs of exfoliated graphene sheets dispersed in ethanol (a), NMP (b), and DMF (c) and approximately 1 g of their respective dried graphene powders (d–f); g) scheme showing the SCF exfoliation of graphite crystals to graphene.

graphite crystals in three different solvents, ethanol, DMF, and NMP, under low-power sonication and heated up to or above their critical temperature. The critical points of the solvents are listed in Table S1 in the Supporting Information. Figure 1g shows the scheme for SCF exfoliation of graphite to GSs. The exfoliation of graphite down to a few layers (< 10 layers) was achieved in SCFs in a shortest reaction time of 15 min. This was possible because of the unique features of the SCFs, such as low interfacial tension, excellent wetting of surfaces, and high diffusion coefficients.[15] These features make SCFs superior solvents for rapid penetration of all the interlayers of graphite with high diffusivity and a solvation power that is much higher than the interlayer energies of graphite. Therefore, our method resulted in a rapid and high-yield conversion of the starting graphite crystals down to 1–10 layer GSs, retaining the original pristine structure of the sheets in one-pot exfoliation.

It is crucial to ascertain the state of the graphite crystals at each stage. Therefore, we have examined the state of the starting graphite crystals, sonicated graphite crystals, and exfoliated graphene sheet by scanning electron microscopy (SEM). The SEM studies showed that the starting graphite powder consisted of flakes approximately 7–25 μm in size, as shown in Figure 2a. After sonication, these larger flakes

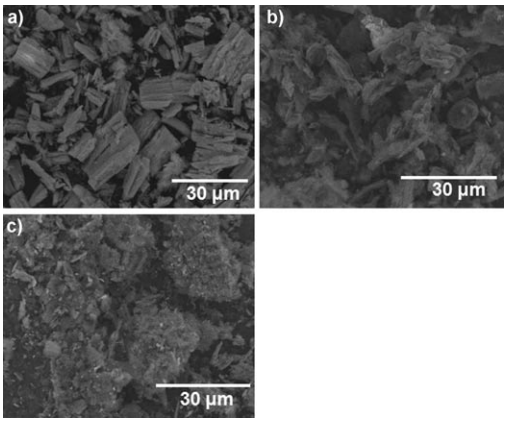

Figure 2. SEM images a) starting graphite crystals, b) ultrasonicated graphite crystals, and c) supercritical ethanol exfoliated graphene sheets.

broke down into smaller flakes approximately 2–10 μm in size (Figure 2b); this shows that sonication resulted in fragmentation of the initial flakes. The effect of sonication is similar to that observed by Hernandez et al.[14] The GSs exfoliated by SCF contain much smaller sheets, 0.1–2 μm in size (Figure 2c). This result clearly indicates that the most of the exfoliation occurred only after SCF treatment as discussed above.

The GSs produced by SCF exfoliation have been characterized by Raman spectroscopy, AFM, and high-resolution (HR) TEM to confirm the exfoliation of the GSs. Raman spectroscopy is a powerful nondestructive technique for identifying the number of layers, structure, doping, and disorder of graphene.[19–21] Raman spectra were recorded with red (633 nm) laser radiation with the dried powder mounted on a glass slide. The typical D (1350), G (1565), and 2D (2650–2690 cm^{-1}) graphitic bands are present in the spectra of all of the exfoliated samples. We observed the D and G bands at approximately 1345 and 1580 cm^{-1}, respectively, for all of the samples (Figure S1 in the Supporting Information). A small D band was also observed for our starting graphite crystals; this indicates that the starting graphite crystals already had small defects. The D-band intensity was slightly increased for the exfoliated GS samples. A relatively small increase in the D-band intensity of GS samples indicates that exfoliated GS samples have less or no defects. Hernandez et al. also reported a small D band in their samples, which were prepared by dispersing graphite in different organic solvents, such as NMP, under sonication. Raman spectra recorded in the 2650–2690 cm^{-1} (2D band) region for all the samples are presented in Figure 3a–c. It is possible to precisely identify the number of layers from the shape and position of 2D band. The spectra showed that all the samples consist of single to few-layered graphene (< 10). We have systematically identified 1–10 layers of GSs in our exfoliated graphene powder samples. Raman spectra of all of the samples agree well with the literature.[19–21] We have employed results from Raman spectroscopy to estimate the yield of exfoliated graphene. The Raman spectra were recorded over 210 spots from 6 different regions of the sample mounted on a glass slide to plot histograms. The total area subjected to the measurements was 2250 μm^2 (Figure S2 in the Supporting Information). About 90–95% of the observed GSs consisted of < 8 layers with a 6–10% monolayer yield and the remaining 5–10% was ≥ 10 layers (Figure 3d–f). This data provides evidence for high-yield exfoliation of graphite crystals to few-layered GSs. It should be noted that, so far, no other methods have provided such an excellent yield of graphene in a direct one-pot conversion. A comparative study has been made on the yield of GSs obtained by our method with a number of other methods reported in the literature (Table S2 in the Supporting Information).

Generally, the achieved exfoliation was typically confirmed by measuring the thickness of a single graphene sheet, which is about 1 nm in height on a substrates such as mica, by using AFM.[10] Therefore, SCF exfoliation of graphite crystals down to a few layers (1–10 layers) was further confirmed by measuring the thickness of the GSs by means of AFM. The representative AFM height images along with height profiles for monolayer graphene sheets are shown in Figure 4a. The height profiles show the steps from the Si to an exfoliated graphene sheet, which is about 0.8 nm for the given cross-section (Figure 4a). Some researchers have reported typical step heights of approximately 0.6–1 nm for single-layer graphene sheets.[14] Hernandez et al. observed a number of graphene monolayers exfoliated by the sonication method with a step height of 1–2 nm.[14] They attributed this large thickness of monolayer to chemical contrast issues and the presence of residual solvent. Since our sample also contains some residual solvent, similar thicknesses can be expected for monolayers rather than the ideal thickness

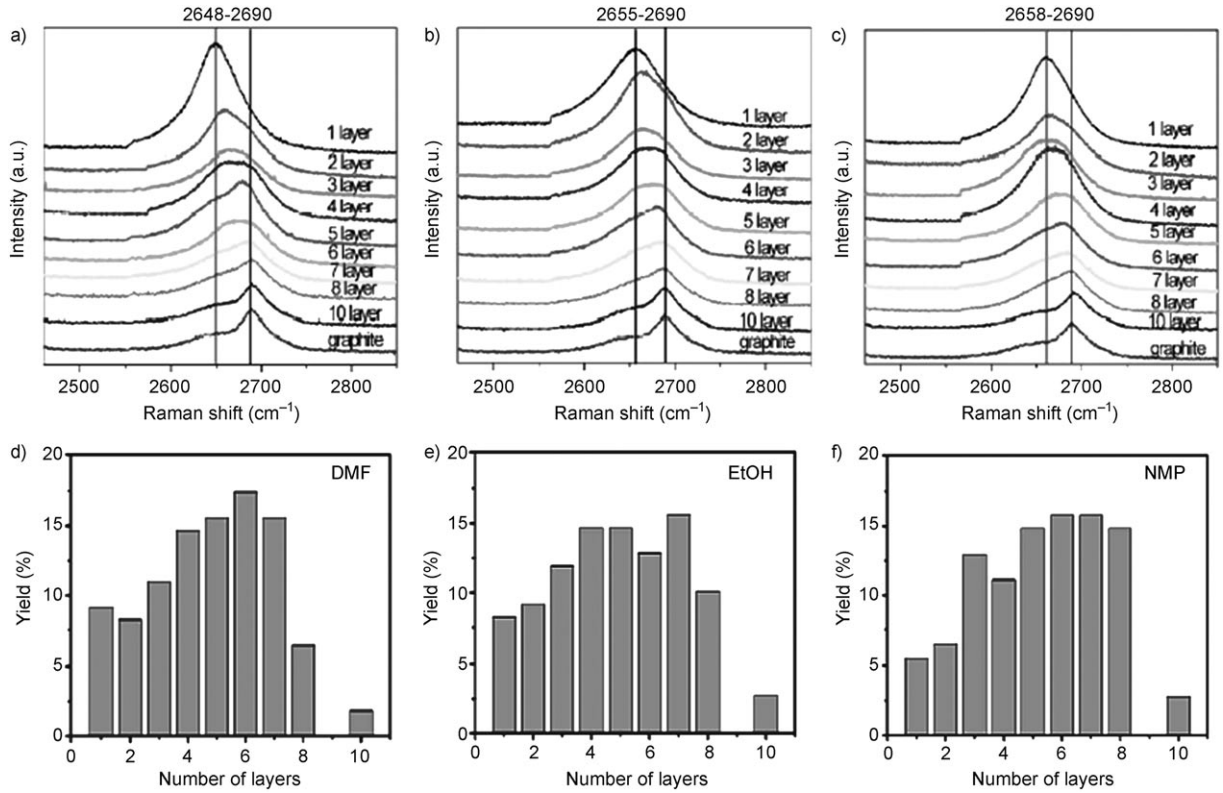

Figure 3. Raman spectra of the 2D band showing 1–10 layer GSs exfoliated by a) DMF, b) EtOH, and c) NMP. The histograms d–f) show the yield of 1–10 layers of GSs in different solvents, respectively.

(0.3 nm) reported by some other methods.[14] We have also observed a thickness corresponding to 3–10 layers of GSs (Figure S3 in the Supporting Information). This observation is consistent with the Raman data presented in Figure 3. Importantly, being a large-scale exfoliation, the GS sample should be thoroughly investigated for the distribution of the number of graphene layers. Normally, in small-scale production, this could be conveniently carried out with AFM measurements. However, in the present study it was realized that, quite often, the graphene layers were overlapping with each other as the AFM specimens were prepared by drop-casting the dispersion of the GSs on a smooth substrate surface. In addition, some graphene sheets were folded due to surface tension during solvent evaporation (Figure S3 in the Supporting Information). This was a major problem that we encountered for the quantitative analysis of the number of layers and conversion yield when using AFM measurements. Such problems can be avoided by using Raman spectroscopy analysis because Raman is agglomeration-blind and considers only interlayer interactions.

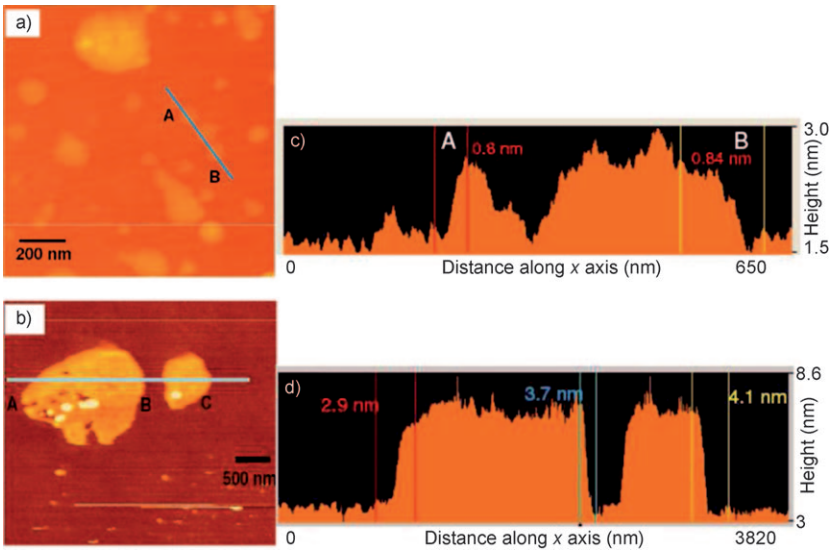

Figure 4. AFM images of graphene sheets exfoliated by a) DMF (1.2×1.2 μm) and the corresponding height profiles at 650 nm (c); and b) ethanol (3.5×2.8 μm) and the height profiles at 3820 nm (d). The height profiles were obtained along the *x* axis from positions A and B/C indicated by the blue lines in AFM images (a) and (b).

Further, the state of dispersed GSs was studied by TEM analysis. The ability to

easily transfer GSs onto the TEM grid allows their detailed characterization by using HR-TEM. The TEM samples were prepared by simply dropping a few drops of dispersed solution onto holey carbon grids (400 mesh). TEM analysis revealed a large quantity of sheets with different types and sizes, as shown in Figure 5. The size of the GS was in the

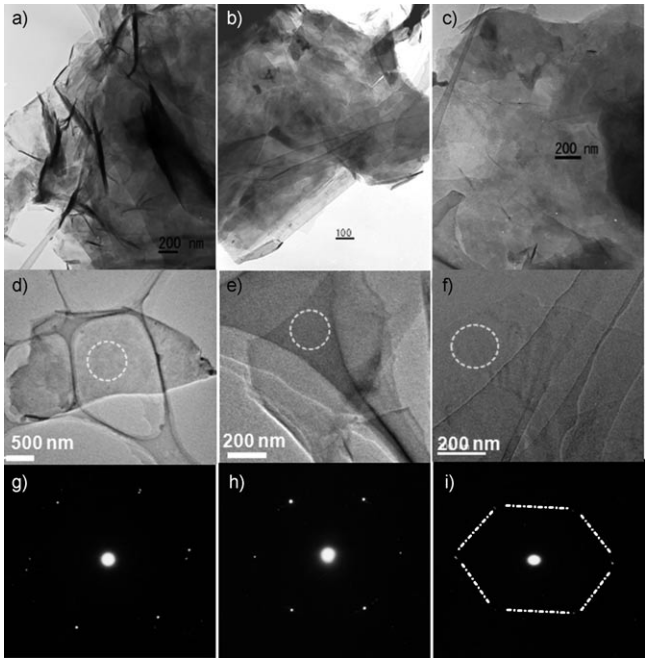

Figure 5. HR-TEM images of GSs exfoliated by a) DMF, b) EtOH, and c) NMP; a–c) several mono- and multilayer GSs; d–f) monolayer GSs, and g–i) the selected area electron diffraction (ED) patterns of the GS showing crystalline graphene structures.

range of several hundred nanometers to two micrometers. Most of the GSs are agglomerated, comprising from mono- to multilayer sheets, as displayed in Figure 5a–c and some of them are only monolayer GSs, as observed in Figure 5d–f. Large flakes were not observed in any of these samples. It should be noted that in the present method we did not employ any flake separation by centrifugation. These TEM images are consistent with Raman analysis that a large proportion of sheets are <8 layers. Electron diffraction (ED) patterns were used to confirm the crystallinity of exfoliated GSs. The ED pattern of our graphene is similar to that reported in the literature, which suggests well-crystallized, one to a few-layered graphene structures (Figure 5g–i).[14,22]

The pristine structure of our exfoliated GSs was further confirmed by powder X-ray diffraction patterns by using the same sample powder that was used for Raman spectroscopy measurements. The XRD patterns of all of the samples showed a characteristic reflection (002) for the exfoliated samples (Figure S4 in the Supporting Information). No shift in the peak position and d spacing of the characteristic reflection (002) indicates that all of the exfoliated samples have retained their original pristine structure. SCF exfoliation did not damage the original pristine structure. However, the peak intensities decreased in the log order for the exfoliated samples. In contrast, the graphene prepared from other routes, such as graphene oxide reduction, GIC exfoliation, and chemically modified graphene resulted in an increase in the d-spacing distance, which shows expansion of the distance between different layers.[23] Samples from these methods show many defects and display poor electrical properties. Graphite exfoliation was carried out under different exfoliation temperatures from 300 to 500 °C by using DMF as the solvent. The results show that, with increasing the exfoliation temperature, the (002) reflection intensity decreased with the increase in the peak width (Figure S4 in the Supporting Information). This indicates that at higher temperatures, the graphene nanosheets were formed and retained their original pristine structure. However, we observed that the temperature above 450 °C was not suitable for exfoliation because DMF decomposes at this temperature and affects the properties of graphene. A detailed study is in progress to confirm the effect of different SCF conditions on the quality and property of exfoliated GSs.

FTIR spectra were measured for the GS powder samples, which were dried in a vacuum oven at 150 °C for 12 h. The FTIR spectra for all samples are shown in Figure S5 in the Supporting Information. All of the spectra are almost featureless, except for one band at 1020–1040 cm^{-1} (Figure S5 in the Supporting Information). This indicates that a small amount of water was absorbed after drying. Therefore, C–O bonding may arise from either tightly bound water molecules or small defective sites in the graphene. This is in contrast to the spectra for graphene oxide published in literature, which contain intense spectral features at around 1700 cm^{-1} that can be attributed to carboxyl groups. Again, this further proves that we produced graphene rather than some form of derivatized graphene.[24]

To study the properties and quality of SCF-exfoliated GSs, we investigated the current–voltage (I–V) characteristics of individual multilayer GSs by using a JEM-3100FEF (JEOL) transmission electron microscope with a piezo-driven TEM–STM holder (Nanofactory),[25,26] as illustrated in Figure 6 with a real TEM image. Typical I–V curves obtained for vacuum-dried GS samples (at 200 °C) show resistance in the range of 2–6 kΩ, as shown in Figure 6c (Table S3 in the Supporting Information). This in fact represents a higher conductivity than the previously reported values for highly conducting GSs, in which a typical resistance for GSs with a channel length of 100 nm at room temperature is 10–30 kΩ[13] (Table 1). A notable feature in our experimental configuration is that the contact area between the W tip and the GS is much smaller than counter gold/GS and lithographically contacted GSs. This further indicates superior electrical conduction due to the high quality of the GS. In addition, the I–V plot clearly exhibits Ohmic behavior in the lower voltage range with a resistance of 2–6 kΩ, which is comparable to that of carbon nanotubes.[26,27] Also, Table 1 clearly indicates that the electrical properties of our GSs are better than the chemically exfoliated GSs reported so

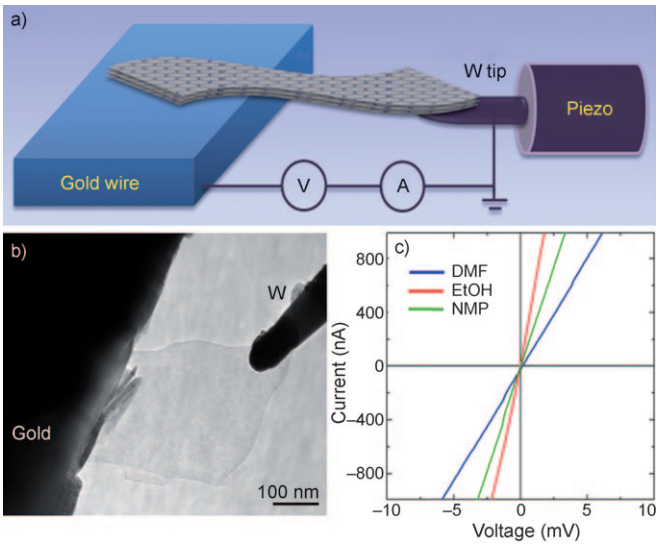

Figure 6. a) Schematic illustration of the TEM experimental setup: a single multilayer graphene sheet has its ends contacted with gold wire and the W tip. b) A TEM image showing nano-graphene connected with the two electrodes inside the TEM–STM holder. c) Typical *I–V* curves obtained for samples in DMF (blue), EtOH (red), and NMP (green) by using the experimental setup and TEM image shown in (a) and (b).

far.[28–31] In a larger voltage range from −2 to 2 V, the *I–V* curve shows nonlinear symmetric behavior and a clear conduction increase in high-bias region (Figure S6a in the Supporting Information). We also measured the maximum current density and stability of the GS by slowly increasing the applied bias on the GS (Table S3 and Figure S7 in the Supporting Information). A single 6-layered GS was finally broken near the W/GS contact at a high current of 1.1 mA. The width of the broken sheet is 65 nm (as indicated by an arrow in Figure S6b in the Supporting Information). If we assume that all layers contribute to electron transport, the estimated current density is at least 1.0×10^9 A cm^{-2}, which is in the same order of magnitude as the best multi-walled CNTs.[26] This result highlights the extremely high stability against electron migration due to the strong sp^2 bonds that are dominant in GS. The good conduction and high current-carrying capacity of GS also suggest that, our GSs are potential candidates for both transistors and interconnect in future nanoelectronic circuits.

Table 1. Comparison of electrical properties of GS prepared in this work with that produced by other chemical approaches.

	Sample	Forms	Electrical properties
1	GS in EtOH	≈5 layers GS	resistance: 2 kΩ
2	GS in DMF	≈6 layers GS	resistance: 1.5–6 kΩ
3	GS in NMP	≈5 layers GS	resistance: 3 kΩ
4	ref. [13]	multilayer Langmuir–Blodgett film	resistance: 8–150 kΩ
5	ref. [29]	drop-cast film on a substrate	resistance: 30.5 kΩ
6	ref. [14]	thin film (≈30 nm thick) on alumina membrane by filtration	conductivity: 65×10^2 S m^{-1}
7	ref. [11]	free-standing paper	conductivity: 6.9×10^2 S m^{-1}
8	ref. [27]	thin evaporated film (≈3 μm thick) on a glass slide	conductivity: 12.5×10^2 S m^{-1}
9	ref. [12]	powder	conductivity: 2×10^2 S m^{-1}
10	ref. [28]	powder	conductivity: $(10–23)\times10^2$ S m^{-1}
11	ref. [26]	single graphene nanoribbon sheet	semiconducting behavior

Conclusion

We have demonstrated a rapid, one-pot SCF process for high-yield exfoliation of GSs. Our procedure is simple and involves direct conversion of graphite crystals to high-quality graphene under SCFs such as ethanol, NMP, and DMF. This is a noncovalent, solution-phase method to produce defect-free, unoxidized graphene with good conduction and electron-carrier capacity. The novel SCF approach allows easy processing and functionalization of GSs by a variety of available techniques and enables its potential use in high performance and scalable applications, such as Li ion batteries, catalysis, and solar cells. Therefore, we believe that the present work would open a gateway for the commercial production of graphene sheets.

Experimental Section

Preparation of exfoliated graphene sheets: All SCF exfoliations were performed in a stainless-steel reactor with a maximum volume of 10 mL. In a typical experiment, graphite crystals (10–20 mg) were added to a stainless-steel reactor vessel and dispersed in a solvent (5 mL), such as ethanol, DMF, or NMP, by low-power sonication (AS ONE US cleaner, US-4R , 40 kHz, 160 W) for 10 min. Then, the sealed reactor vessel was heated to 300–400 °C for 15–60 min in a specially designed tube furnace (AKICO, Japan). The reactor reaches the optimum temperature within 3 min, therefore, the reaction time mentioned above includes the ramp up time. The pressure was maintained at 38–40 MPa by adjusting the volume and temperature of the reactor vessel. The reaction was terminated by submerging the hot reactor in an ice-cold water bath. The exfoliated GSs were collected by repeatedly washing and centrifuging with fresh solvent and were then vacuum dried overnight at 100 °C.

Characterization of graphene sheets: Raman spectra were recorded in the backward geometry on a NIHON BUNKO Ventuno spectrometer (NSR-1000DT) at room temperature. The powder sample was excited by using the 632.8 nm wavelength line from a He–Ne laser. Scans were taken on an extended range of (400–3500 cm^{-1}) with an exposure time of 30 s. The dried GS powder was pressed on a glass slide for observation. The sample was viewed by using a red laser apparatus under the maximum magnification of ×100. The AFM measurements were performed with an S-image, Multi-Function unit. Graphene suspensions were applied directly on the substrate, which was a thin native oxide on Si (100), by a drop-casting method. After drying the substrate in a clean environment at room temperature, the measurements were performed in air at ambient temperature and pressure. The HR-TEM images were obtained with a HRTEM JEOL JEM-2010F instrument. The TEM samples were prepared by simply dropping a few drops of dispersed GS solution on to holey carbon grids (400 mesh). The structure was examined by XRD analysis with a

Bruker AXS D8 Advance instrument using $Cu_{K\alpha}$ radiation. IR spectra of the GS were recorded by using an FT/IR-6200 IR spectrophotometer (JASCO Corp., Tokyo, Japan).

Electron transport experiments: The electron transport experiments were carried out by in situ measurement using a JEM-3100FEF (JEOL) transmission electron microscope with a piezo-driven TEM–STM holder (Nanofactory). A two-terminal connection was made to individual nanographene sheets by contacting both ends with two metal electrodes. First, a freshly cut gold wire (0.25 mm in diameter) was inserted into the microhole on a gold "hat" (Figure 6 a and b). Then, the wire tip was delicately immersed into graphene powder and then the hats with the sample-holding wires were mounted on a sapphire ball of the piezo-driven tubes of the TEM–STM holder. It was noted that during sample deposition the graphene sheets were attracted to the gold wires due to simple adhesion forces. No organic glues or pastes were used for sample assembly to avoid electrical/mechanical circuit contamination. The counterparts of the holders consisted of a tungsten tip prepared by an electrochemical etching method and inserted into the three-dimensional movable part of the piezo-driven holder. This tungsten tip was then controlled to approach the graphene sheets under TEM observation. As shown in Figure 6a, a single multilayer graphene nanosheet protruding from the edge of the gold wire was brought into contact with a tungsten tip.

Acknowledgements

This research is partially supported by Japan Society for the Promotion of Science (JSPS) and New Energy and Industrial Technology Development Organization (NEDO). The authors wish to thank Dr. Yoshio Bando, National Institute for Materials Science, for STM–TEM measurements and Prof. Tetsuichi Kudo for fruitful discussions.

[1] a) A. K. Geim, K. S. Novoselov, *Nat. Mater.* **2007**, *6*, 183–191; b) M. S. Dresselhaus, G. Dresselhaus, *Adv. Phys.* **2002**, *51*, 1; c) A. D. Dmitriy, S. Sasha, J. Z. Eric, D. P. Richard, H. B. Geoffrey, G. E. Dommett, T. N. SonBinh, S. R. Rodney, *Nature* **2007**, *448*, 457; d) I. Forbeaux, J. M. Themlin, J.-M. Debever, *Phys. Rev. B* **1998**, *58*, 16396; e) C. N. R. Rao, K. Biswas, K. S. Subrahmanyam, A. Govindaraj, *J. Mater. Chem.* **2009**, *19*, 2457.

[2] K. S. Novoselov, D. Jiang, F. Schedin, T. J. Booth, V. V. Khotkevich, S. V. Morozov, A. K. Geim, *Proc. Natl. Acad. Sci. USA* **2005**, *102*, 10451–10453.

[3] C. Berger, Z. Song, X, Li, X. Wu, N. Brown, C. Naud, D. Mayou, T. Li, J. Hass, A. N. Marchenkov, E. H. Conrad, P. N. First, W. A. de Heer, *Science* **2006**, *312*, 1191–1196.

[4] T. Ohta, F. E. Gabaly, A. Bostwick, J. L. McChesney, K. V. Emtsev, A. K. Schmid, T. Seyller, K. Horn and E. Rotenberg, *New J. Phys.* **2008**, *10*, 023034.

[5] C. Berger, Z. M. Song, T. B. Li, X. B. Li, A. Y. Ogbazghi, R. Feng, Z. T. Dai, A. N. Marchenkov, E. H. Conrad, P. N. First, W. A. de Heer, *J. Phys. Chem. B* **2004**, *108*, 19912–19916.

[6] A. Dato, V. Radmilovic, Z. Lee, J. Phillips, M. Frenklach, *Nano Lett.* **2008**, *8*, 2012–2016.

[7] J. J. Wang, M. Y. Zhu, R. A. Outlaw, X. Zhao, D. M. Manos, B. C. Holloway, V. P. Mammana, *J. Appl. Phys. Lett.* **2004**, *85*, 1265–1267.

[8] J. Campos-Delgado, J. M. Romo-Herrera, X. Jia, D. A. Cullen, H. Muramatsu, Y. A. Kim, T. Hayashi, Z. Ren, D. J. Smith, Y. Okuno, T. Ohba, H. Kanoh, K. Kaneko, M. Endo, H. Terrones, M. S. Dresselhaus, M. Terrones, *Nano Lett.* **2008**, *8*, 2773–2778.

[9] M. Choucair, P. Thordarson, J. A. Stride, *Nat. Nanotechnol.* **2009**, *4*, 30–33.

[10] S. Park S, R. S. Ruoff, *Nat. Nanotechnol.* **2009**, *4*, 217–224.

[11] S. Park, J. An, R. D. Piner, I. Jung, D. Yang, A. Velamakanni, S. B. T. Nguyen R. S. Ruoff, *Chem. Mater.* **2008**, *20*, 6592–6594.

[12] S. Stankovich, D. A. Dikin, R. Piner, K. M. Kohlhaas, A. Kleinhammes, Y. Jia, Y. Wu, S. T. Nguyen, R. S. Ruoff, *Carbon* **2007**, *45*, 1558–1565.

[13] X. Li, G. Zhang, X. Bai, X. Sun, X. Wang, E. Wang, H. Dai, *Nat. Nanotechnol.* **2008**, *3*, 538–542.

[14] a) Y. Hernandez, V. Nicolosi, M. Lotya, F. M. Blighe, Z. Sun, S. De, I. T. McGovern, B. Holland, M. Byrne, Y. Gun'ko, J. Boland, P. Niraj, G. Duesberg, S. Krishnamurthy, R. Goodhue, J. Hutchison, V. Scardaci, A. C. Ferrari, J.N Coleman, *Nat. Nanotechnol.* **2008**, *3*, 563–568; b) S. Stankovich, D. A. Dikin, G. H. B. Dommett, K. M. Kohlhaas, E. J. Zimney, E. A. Stach, R. D. Piner, S. T. Nguyen, R. S. Ruoff, *Nature* **2006**, *439–444*, 7100.

[15] a) G. K. Serhatkulu, C. Dilek, E. Gulari, *J. Supercrit: Fluids* **2006**, *39*, 264–270; b) E. Gulari, G. K. Serhatkulu, US patent application 20,050,014,867, **2003**; c) K. P. Johnston, P. S. Shah, *Science* **2004**, *303*, 482–483.

[16] M. Sathish, K. Miyazawa, J. P. Hill and K. Ariga, *J. Am. Chem. Soc.* **2009**, *131*, 6372–6373.

[17] a) C. A. Furtado, U. J. Kim, H. R. Gutierrez, Ling Pan, E. C. Dickey, and Peter C. Eklund, *J. Am. Chem. Soc.* **2004**, *126*, 6095–6105; b) S. Giordani, S. D. Bergin, V. Nicolosi, S. Lebedkin, M. M. Kappes, W. J. Blau, J. N. Coleman, *J. Phys. Chem. B* **2006**, *110*, 15708–15718.

[18] T. Hasan, V. Scardaci, P. H. Tan, A. G. Rozhin, W. I. Milne, A. C. Ferrari, *J. Phys. Chem. C* **2007**, *111*, 12594–12602.

[19] A. Gupta, G. Chen, P. Joshi, S. Tadigadapa, P. C. Eklund, *Nano Lett.* **2006**, *6*, 2667–2267.

[20] A. C. Ferrari, *Solid State Commun.* **2007**, *143*, 47–57.

[21] A. Das, S. Pisana, B. Chakraborty, S. Piscanec, S. K. Saha, U. V. Wagmare, K. S. Novselov, H. R. Krishanamurthy, A. K. Geim, A. C. Ferrari, A. K. Sood, *Nat. Nanotechnol.* **2008**, *3*, 210–215.

[22] M. Lotya, Y. Hernandez, P. J. King, R. J. Smith, V. Nicolosi, L. S. Karlsson, F. M. Blighe, S. De, Z. Wang, I. T. McGovern, G. S. Duesberg, J. N. Coleman, *J. Am. Chem. Soc.* **2009**, *131*, 3611–3620.

[23] a) M. J. McAllister, J-L. Li, D. H. Adamson, H. C. Schniepp, A. A. Abdala, J. Liu, M. H. Alonso, D. L. Milius, R. Car, R. K. Prud'homme, I. A. Aksay, *Chem. Mater.* **2007**, *19*, 4396–4404; b) J. Shen, Y. Hu, C. Li, C. Qin, M. Ye, *Small* **2009**, *5*, 82–85.

[24] a) Y. Si, E. T. Samulski, *Nano Lett.* **2008**, *8*, 1679–1682; b) S. Park, J. An, R. D. Piner, I. Jung, D. Yang, A. Velamakanni, S. T. Nguyen, R. S. Ruoff, *Chem. Mater.* **2008**, *20*, 6592–6594.

[25] D. Golberg, M. Mitome, K. Kurashima, C. Y. Zhi, C. C. Tang, Y. Bando, O. Lourie, *Appl. Phys. Lett.* **2006**, *88*, 123101.

[26] M. S. Wang, J. Y. Wang, Q. Chen, L. M. Peng, *Adv. Funct. Mater.* **2005**, *15*, 1825.

[27] B. Q. Wei, R. Vajtai, P. M. Ajayan, *Appl. Phys. Lett.* **2001**, *79*, 1172–1174.

[28] X. Li, X. Wang, L. Zhang, S. Lee, H. Dai, *Science* **2008**, *319*, 1229–1232.

[29] Y. Si, E. T. Samulski, *Nano Lett.* **2008**, *8*, 1679–1682.

[30] M. J. McAllister, J. L. Li, D. H. Adamson, H. C. Schniepp, A. A. Abdala, J. Liu, M. H. Alonso, D. L. Milius, R. Car, R K. Prud′homme, I. A. Aksay, *Chem. Mater.* **2007**, *19*, 4396–4404.

[31] G. Williams, B. Serger, P. V. Kamat, *ACS Nano* **2008**, *2*, 1487–1491.

Received: January 25, 2010
Published online: April 22, 2010

